Ligand-Independent Androgen Receptor Variants Derived from Splicing of Cryptic Exons Signify Hormone-Refractory Prostate Cancer

Rong Hu,[1] Thomas A. Dunn,[1] Shuanzeng Wei,[1] Sumit Isharwal,[1] Robert W. Veltri,[1] Elizabeth Humphreys,[1] Misop Han,[1] Alan W. Partin,[1,3] Robert L. Vessella,[4] William B. Isaacs,[1,2,3] G. Steven Bova,[1,2,3] and Jun Luo[1,2]

Departments of [1]Urology, [2]Oncology, and [3]Pathology, The Johns Hopkins University School of Medicine, Baltimore, Maryland and [4]Department of Urology, University of Washington and the Puget Sound VA Medical Center, Seattle, Washington

Abstract

Suppression of androgen production and function provides palliation but not cure in men with prostate cancer (PCa). Therapeutic failure and progression to hormone-refractory PCa (HRPC) are often accompanied by molecular alterations involving the androgen receptor (AR). In this study, we report novel forms of AR alteration that are prevalent in HRPC. Through *in silico* sequence analysis and subsequent experimental validation studies, we uncovered seven AR variant transcripts lacking the reading frames for the ligand-binding domain due to splicing of "intronic" cryptic exons to the upstream exons encoding the AR DNA-binding domain. We focused on the two most abundantly expressed variants, AR-V1 and AR-V7, for more detailed analysis. AR-V1 and AR-V7 mRNA showed an average 20-fold higher expression in HRPC (n = 25) when compared with hormone-naive PCa (n = 82; P < 0.0001). Among the hormone-naive PCa, higher expression of AR-V7 predicted biochemical recurrence following surgical treatment (P = 0.012). Polyclonal antibodies specific to AR-V7 detected the AR-V7 protein frequently in HRPC specimens but rarely in hormone-naive PCa specimens. AR-V7 was localized in the nuclei of cultured PCa cells under androgen-depleted conditions, and constitutively active in driving the expression of canonical androgen-responsive genes, as revealed by both AR reporter assays and expression microarray analysis. These results suggest a novel mechanism for the development of HRPC that warrants further investigation. In addition, as expression markers for lethal PCa, these novel AR variants may be explored as potential biomarkers and therapeutic targets for advanced PCa. [Cancer Res 2009;69(1):16–22]

Introduction

Prostate cancer (PCa) depends on androgenic signaling for growth and survival. Androgens exert their cellular and physiologic effects through binding to the androgen receptor (AR), a member of the steroid hormone receptor family of transcription factors (1). The human *AR* gene is located on chromosome Xq11-12 and spans ~180 kb of DNA with eight known exons. The prototype AR protein contains several functional domains (2). The NH_2-terminal domain (NTD), encoded by exon 1, constitutes ~60% of the 110-kDa full-length protein and is the transcriptional regulatory region of the protein. The central DNA-binding domain (DBD) is encoded by exons 2 and 3, whereas exons 4 to 8 code for the COOH-terminal ligand-binding domain (LBD). Androgen binding to the AR LBD allows entry of the ligand-bound receptor into the nucleus and subsequent transcriptional regulation of androgen-responsive genes (3). Hormonal therapies for advanced PCa target AR-mediated functions by suppressing the production of androgens and/or androgen binding to the AR LBD. Although these therapies often result in a period of clinical regression, they are not curative due to progression to hormone-refractory PCa (HRPC) for which effective therapeutic options are limited (4).

AR-mediated functions are not completely abrogated by the existing hormone therapies. HRPC continues to depend on AR-mediated functions but bypasses the requirement for physiologic levels of androgens (5, 6). Molecular alterations involving AR itself, such as AR overexpression and gain-of-function AR LBD mutations, are common in HRPC and allow for continued AR-mediated genomic functions under the presence of reduced or altered ligands (5, 6). Despite the established clinical relevance of these well-characterized AR alterations in HRPC, a few previous studies have suggested an alternative mechanism for HRPC and investigated the putative role of AR variants lacking the AR LBD (ARΔLBD; refs. 7, 8). These variants, arising from somatic nonsense mutations (7), or post-translational AR proteolysis (8), were functionally active in the absence of androgens (7, 8). Although cellular production of such ARΔLBD isoforms seems to be most effective in achieving complete androgen independence, their precise origins and relevance to HRPC were less well substantiated. In a recent study, Dehm and colleagues (9) used the rapid amplification of cDNA ends technique and reported a novel exon within AR intron 2. Splicing of this novel exon introduced a premature stop codon upstream of exon 3 in the AR transcript that would encode an AR protein lacking the second zinc finger of the DBD and LBD if translated (9). In the present study, we performed a comprehensive *in silico* sequence analysis of the human AR genomic locus and uncovered multiple novel ARΔLBD variants with intact coding potential for the full AR NTD and AR DBD. These novel AR transcripts were overexpressed in HRPC and one of the most abundant variants, AR-V7, was expressed at elevated levels in a subset of hormone-naive PCa that recurred after surgical treatment. Moreover, for the first time, we generated variant-specific antibody against the LBD-truncated AR-V7 and detected this AR variant protein frequently in HRPC specimens. The expression pattern and the validated androgen-independent function of these novel AR variants potentially added another level of detail to the molecular mechanism of HRPC that could ultimately affect the management of patients with advanced PCa.

Requests for reprints: Jun Luo, Department of Urology, The Johns Hopkins University School of Medicine, 411 Marburg Building, 600 North Wolfe Street, Baltimore, MD 21287. Phone: 443-287-5625; Fax: 410-502-9336; E-mail: jluo1@jhmi.edu.

doi:10.1158/0008-5472.CAN-08-2764

Materials and Methods

Human prostate tissue samples. Hormone-naive prostate tissue specimens used in this study (n = 82) were collected and fresh frozen at the time of radical retropubic prostatectomy (RRP), from 1993 to 2001, at the Johns Hopkins Hospital. Prostate specimens were processed as described previously before RNA extraction (10). HRPC specimens were either collected at the time of the transurethral resection of the prostate (TURP) operation in patients who failed hormone therapies (n = 4) or metastatic HRPC tissues (n = 21) collected from 20 patients who died from PCa, as part of the Johns Hopkins Autopsy Study of lethal PCa (Supplementary Table S1; ref. 11). The use of surgical and autopsy specimens for molecular analysis was approved by the Johns Hopkins Medicine Institutional Review Boards.

Cloning and sequencing of AR variants. First-strand cDNA synthesis was performed using 500 ng total RNA, 0.5 μg oligo(dT), and 200 units of SuperScript II reverse transcriptase (Invitrogen) in a volume of 20 μL. PCR products derived from the primer pairs (Supplementary Table S2) were cloned into TopoTA vector (Invitrogen) and subjected to sequencing analysis using the Applied Biosystems 3730x1 DNA analyzer. To facilitate the amplification and sequencing of GC-rich AR NTD, DMSO (10%) was added in the PCR for full-length variant cloning and subsequent sequencing analysis.

AR variant mRNA expression analysis. For semiquantitative reverse transcription-PCR (RT-PCR) analysis, 2.5% of the cDNA product from 500 ng input total RNA was used for each sample and each transcript. For real-time quantitative RT-PCR, 0.125% of the cDNA product was used in the iQ SYBR Green Supermix assays (Bio-Rad). Given the highly variable expression of many genes among clinical specimens, we analyzed previously published expression microarray data and identified SF3A3, which encodes a splicing factor, as a reference gene for normalization due to its stable expression levels among various prostate specimens, including HRPC, primary PCa, normal prostate samples, and cell lines (12). Only primer pairs with validated amplification specificity were used (Supplementary Table S2). Following validation of equal amplification efficiencies for both target transcripts and SF3A3, the average threshold cycle (C_t) numbers from reactions run in triplicate were used for comparative threshold analysis. For presentation purposes and for comparison among different figures, all expression values were $\log_2$ transformed with measurable values for the RRP cases centered at zero.

AR variant protein analysis. Whole-cell lysates were prepared using radioimmunoprecipitation assay buffer (Pierce) according to the vendor's recommendations. Nuclear and cytosolic extracts were prepared using the Nuclear and Cytoplasmic Extraction Reagents (Pierce). Protein samples were resolved on 4% to 12% gradient SDS-PAGE gels and subjected to standard immunoblot analysis with anti-AR(N20) (Santa Cruz Biotechnology), anti-AR-V7, or anti-β-actin (Sigma-Aldrich) antibodies. The mouse polyclonal anti-AR-V7 antibody was developed using the COOH-terminal peptide (CKHLKMTRP) specific to the AR-V7 protein by a commercial vendor (A&G Pharmaceutical). For immunoprecipitation (IP), a total of 300 μg input whole-cell lysates from cell lines or human tissues was precipitated with 4 μg of monoclonal anti-AR(441) (Santa Cruz Biotechnology) or control mouse IgG, followed by the addition of protein G-agarose (GE Healthcare), and subjected to standard immunoblot analysis.

Luciferase reporter assay. pEGFP-AR and pEGFP-Q640X, which contain the full-length prototype AR and AR Q640X LBD-truncated mutant cDNA, were kind gifts of Dr. Jocelyn Céraline (Université Strasbourg, Strasbourg, France). The cDNA encoding the full-length AR-V7 was inserted into the pEGFP-C3 vector to express the GFP-AR-V7 fusion protein. Each of these constructs was cotransfected together with the PSAP1 luciferase reporter plasmid and pRL-CMV plasmid, an internal *Renilla* luciferase transfection control. Transfected cells were cultured in phenol red–free RPMI 1640 containing 10% charcoal-stripped serum (CSS) for 24 h and cultured for another 24 h in the presence or absence of R1881 (NEN) before being harvested and subjected to the Dual-Luciferase Reporter Assay (Promega).

Statistical analysis. All data were analyzed using Stata v10.0 statistical analyses software (Stata Corp.). The Mann-Whitney test was used to evaluate distribution difference across two groups. Cox proportional hazard regression was used to identify significant prognostic factors for prediction of PCa progression-free survival. The proportional hazard assumption was verified by examination of residual plots and Schoenfeld residuals. Log rank was used to test equality of survivor functions across two groups. Statistical significance in this study was set as $P \leq 0.05$.

Results and Discussion

Identification of cryptic AR exons. We performed BLAST searches of the ~170-kb AR intron sequences against the National Center for Biotechnology Information human expressed sequence tag database. High quality hits (99% identity) were found in intron 1 (6 hits), intron 2 (3 hits), and intron 3 (3 hits) but not in the remaining four introns (Supplementary Table S3). These transcribed "intronic" genomic fragments, considered as putative cryptic exons, were not spliced as currently annotated, and therefore, their exon-intron junctions were undefined. Because a functional AR would most likely retain the AR DBD encoded by exons 2 and 3, we focused on the three putative cryptic exons in intron 3 to determine whether and how they were joined (i.e., spliced) with the upstream exon 3, and their potential to disrupt the AR open reading frame (ORF). We designed primers (P1, P2, and P3; Supplementary Table S2) to amplify and sequence mRNA transcripts containing exons encoding AR DBD and the putative cryptic exons. The detection and subsequent sequencing of the amplicons derived from the CWR22Rv1 cells confirmed that all three cryptic exons (CE1, CE2, and CE3) were joined with exon 3 (Fig. 1*A*). These sequencing results were used to construct seven AR transcript variants, named AR-V1 to AR-V7, each containing one of the three original cryptic exons (Fig. 1*A*). Analysis of transcripts containing cryptic exon 1 (CE1) also uncovered an additional cryptic exon in intron 2, named CE4 (Fig. 1*A*), which was spliced in both AR-V3 and AR-V4 (Fig. 1*A*). The genomic position of CE4 is identical to the novel exon recently published by Dehm and colleagues (9), but the specific sequence reported differed from the consensus sequences we detected in the two CE4-containing variants (AR-V3 and AR-V4; Fig. 1*A*). CWR22Rv1 is a human PCa cell line derived from a serially transplanted PCa xenograft that relapsed after castration-induced regression and is known to have a unique duplicated exon 3 (13). The duplicated exon 3 was reflected in AR-V2 and AR-V4 transcripts (Fig. 1*A*). AR-V5 and AR-V6 contained cryptic exon 2 (CE2) and differed by a contiguous 80-bp sequence at the 5′ junction of CE2 due to alternative 5′ splicing sites spaced 80 bp apart in CE2 (data not shown). Of importance, all seven AR variants harbor premature termination codons (PTC) downstream of AR DBD, generating AR LBD-truncated AR proteins if translated (Fig. 1*A*).

Cloning of the full-length ORFs of AR-V1 and AR-V7. Semiquantitative RT-PCR analysis in a small set of clinical specimens detected the variant transcripts prevalently in HRPC samples (Fig. 1*B*). The full-length ORFs of AR-V1 and AR-V7 were then amplified from two clinical HRPC specimens and CWR22Rv1 cells (Fig. 1*C*). Sequence analysis of the full-length amplicons confirmed the intact ORF of AR NTD and DBD and, thus, the transcript structure for AR-V1 and AR-V7. Due to their relative lower abundance (Fig. 1*B*), AR-V5 and AR-V6 were not further pursued for full-length ORF cloning. AR-V2 and AR-V4 were specific to CWR22Rv1 (data not shown) due to the presence of exon 3 duplication and therefore also not pursued further. AR-V3 harbors a stop codon in CE4 and would lack the second zinc finger of AR DBD encoded by exon 3. Such variants may not be functional

according to a previous study (14), although the study by Dehm and colleagues (9) suggested otherwise. In addition, the full-length ORF for AR-V3 thus far has not been detected in sequenced clones (data not shown). For these reasons, only AR-V1 and AR-V7 were pursued further.

Expression analysis of AR-V1 and AR-V7. HRPC specimens expressed consistently higher levels of AR-V1, AR-V7, and the prototype AR detected using optimized primer sets specific to each target transcript (Fig. 2*A*). Expression of the prototype AR can be readily detected at 28 PCR cycles, whereas detection of the AR

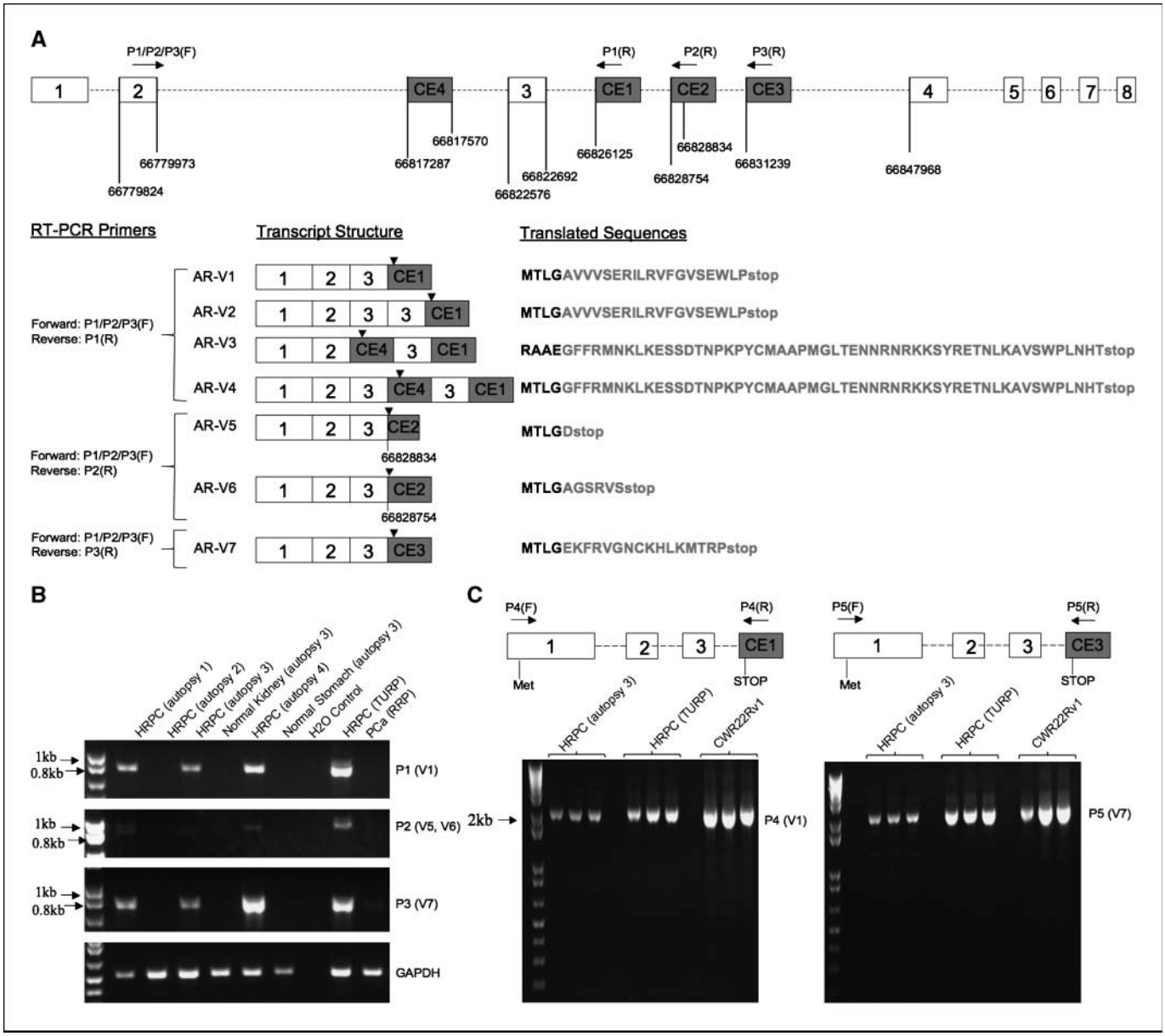

Figure 1. Cloning of novel AR variants. *A,* novel AR variants lacking LBD generated by splicing of four cryptic exons. The eight canonical exons of the *AR* gene were represented by numbered open boxes and shown (not to scale) in relation to the genomic positions of the four cryptic exons (CE1 to CE4) in shaded boxes. The identical forward primer, P1/P2/P3(F), in exon 2 was paired with three reverse primers (P1R, P2R, and P3R; Supplementary Table S2) designed based on Genbank entries for the three transcribed genomic fragments in intron 3 (Supplementary Table S3). Sequencing of the amplicons (from CWR22Rv1 cells) defined the 5′ junctions of CE1, CE2, and CE3, and 5′ and 3′ junctions of CE4, as marked by vertical lines with the corresponding genomic coordinates (Human Genome Assembly March 2006, HG18). Note that there were four CE1-containing variants (AR-V1, AR-V2, AR-V3, and AR-V4) and that the two CE2-containing variants (AR-V5 and AR-V6) differed by an 80-bp contiguous 5′ extension in CE2. Stop codons were marked with the arrowheads in the schematically illustrated transcripts. The seven translated protein sequences corresponding to the seven transcripts were shown, starting from the last four amino acids encoded by exon 3 (AR-V1, AR-V2, AR-V4, AR-V5, AR-V6, and AR-V7) or exon 2 (AR-V3), and followed by variable lengths of variant-specific sequences in light gray that matched the cryptic exons. *B,* detection of the AR variant transcripts by semiquantitative RT-PCR in clinical prostate specimens using the same sets of P1, P2, and P3 primers. Note that AR-V3, with expected size of 1,126 bp by P1 primer set (Supplementary Table S2), was not detected in these clinical specimens. *HRPC (autopsy),* metastatic HRPC samples from autopsies; *HRPC (TURP),* HRPC samples from TURP; *PCa (RRP),* hormone-naive PCa from RRP specimens. *C,* amplification of full-length coding region for AR-V1 and AR-V7 using primer sets P4 and P5 (Supplementary Table S2) from one HRPC autopsy sample, one TURP sample, and the CWR22Rv1 cell line. Identical forward primers, P4(F) and P5(F) located upstream of the translation start codon in exon 1, were paired with reverse primers, P4(R) and P5(R), located downstream of the stop codon in cryptic exon 1 and cryptic exon 3.

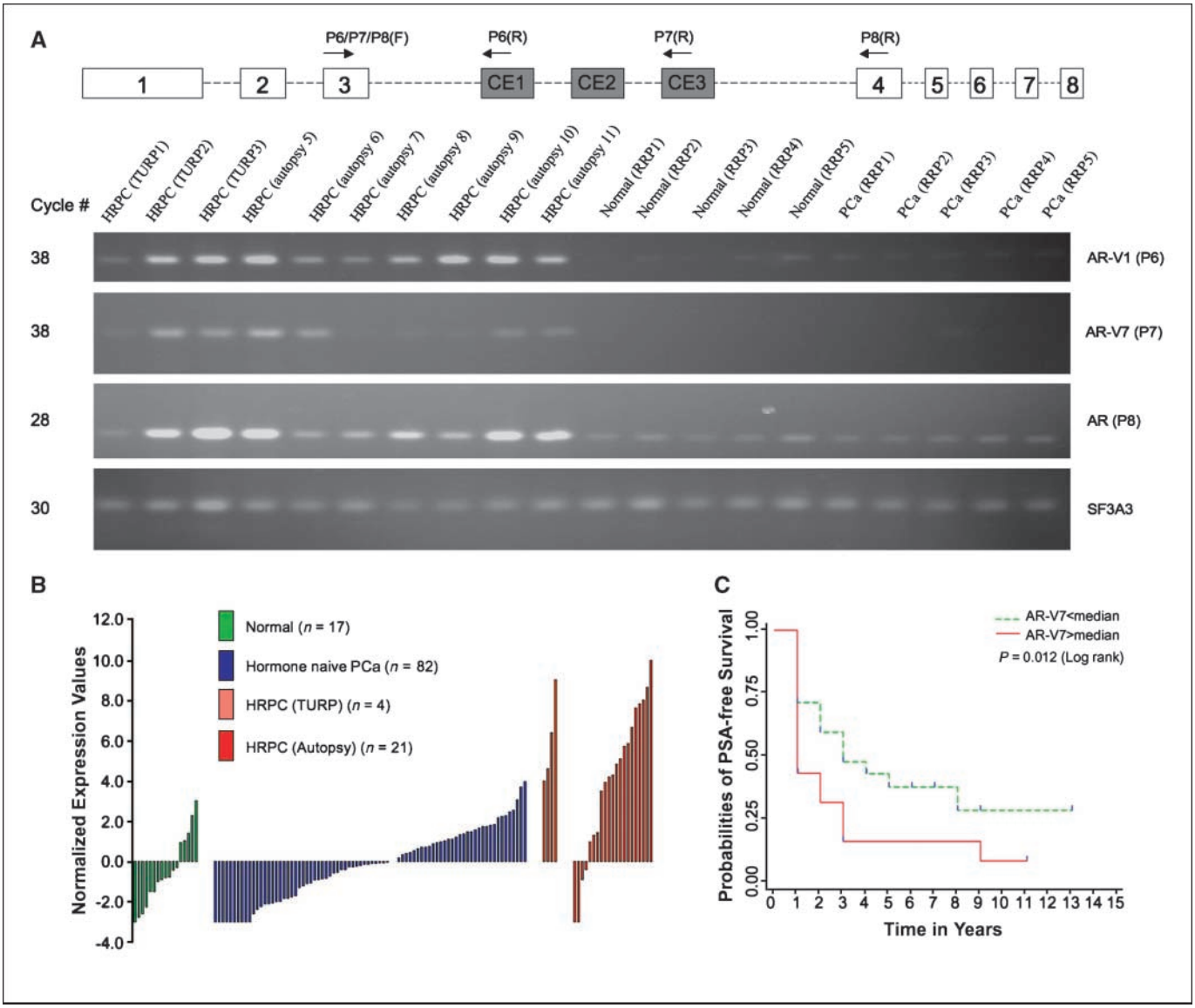

Figure 2. Quantification of AR variant transcripts in clinical specimens. *A,* representative gel images of amplified AR variant transcripts detected using primer sets designed for real-time RT-PCR assays. An identical forward primer, P6/P7/P8(F), in exon 3 was paired with different reverse primers, P6(R), P7(R), and P8(R) (Supplementary Table S2), to amplify the AR-V1, AR-V7, and prototype AR transcripts, respectively. SF3A3 was used as a reference gene transcript (Materials and Methods). *Normal (RRP),* normal prostate tissues from RRP specimens; *PCa (RRP),* hormone-naive PCa from RRP specimens; *HRPC (TURP),* HRPC samples from TURP; *HRPC (autopsy),* metastatic HRPC samples from autopsies (Supplementary Table S1). *B,* quantitative results of AR-V7 in 124 clinical prostate specimens by real-time PCR. Normalized expression values (in $\log_2$ scale) for AR-V7 derived from comparative threshold analysis were shown in four groups of clinical specimens. *Normal (n = 17),* normal prostate tissues from RRP specimens; *Hormone naive PCa (n = 82),* PCa samples from RRP specimens; *HRPC (TURP) (n = 4),* HRPC samples from TURP; *HRPC (autopsy) (n = 21),* metastatic HRPC samples from autopsies (Supplementary Table S1). *C,* Kaplan-Meier plot comparing progression-free survival in patients with less than median AR-V7 expression (n = 38) with those with greater than median AR-V7 expression (n = 28). The survival curves were compared using the log-rank test. Follow-up years were marked on the *X* axis. Censored subjects were marked with vertical ticks in blue. Note that the PSA recurrence status was annotated in years, not months.

variants required 38 cycles, suggesting the lower abundance of the AR variants, at mRNA levels, relative to the prototype AR (Fig. 2*A*). Quantitative real-time RT-PCR of AR-V1, AR-V7, and prototype AR was performed on an expanded series of human prostate tissues (n = 124) and cell lines (n = 9; Supplementary Fig. S1). Expression levels of AR-V1, AR-V7, and prototype AR were significantly higher in HRPC (n = 25) than in hormone-naive PCa (n = 82; P < 0.0001, Mann-Whitney test). Adjusted for amplification efficiency, the average expression values for prototype AR (Supplementary Fig. S2*A*), AR-V1 (Supplementary Fig. S2*B*), and AR-V7 (Fig. 2*B*) were elevated by 11-, 22-, and 20-fold, respectively, when compared with hormone-naive PCa. It is unlikely that nuclear splicing intermediates of the prototype AR gene contributed to the detected AR variant signals because nRNA contributed <5% of the signal when compared with cytoplasmic RNA on a per cell basis (Supplementary Fig. S3). A subset of hormone-naive PCa expressed AR variants at levels comparable with those in HRPC specimens (Fig. 2*B*). This elevated AR-V7 expression was associated with worse clinical outcome (log-rank P = 0.012), as defined by prostate-specific antigen (PSA) recurrence following surgical treatment

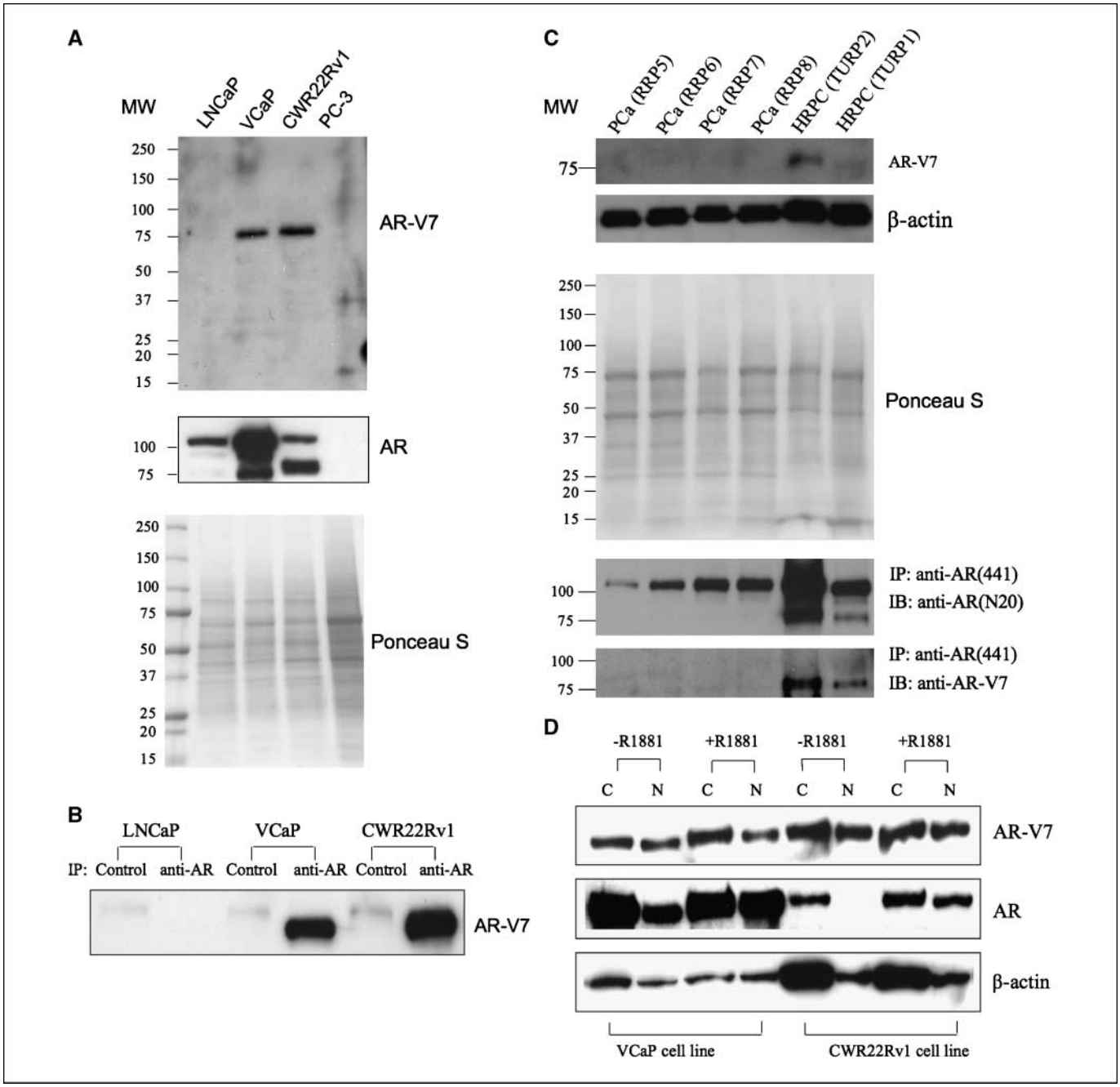

Figure 3. AR-V7 protein detection and analysis using a variant-specific antibody. *A,* detection of AR-V7 protein product in cell lines expressing high levels of AR-V7 transcript (Supplementary Fig. S1). Following immunoblot analysis for AR-V7 (*top*), the same membrane was stripped and subjected to immunoblot analysis with anti-AR(N20) antibody (*middle*) to detect the prototype AR. *Bottom,* loading of total protein was monitored by Ponceau S staining of the polyvinylidene difluoride (PVDF) membrane. *B,* detection of AR-V7 protein following enrichment of all NTD-containing AR proteins by IP using the anti-AR(441) antibody. Note that following enrichment, AR-V7 was detected in cell lines expressing highest levels of AR-V7 mRNA, VCaP and CWR22Rv1 cells, but not in LNCaP cells, which expressed low levels of AR-V7 (Supplementary Fig. S1). *Control,* mouse IgG; *anti-AR,* anti-AR(441) monoclonal antibody. *C,* detection of AR-V7 protein in HRPC. Western blot analysis was performed to detect AR-V7 in whole tissue lysates and enriched AR protein extracts derived from four hormone-naive human PCa tissue (RRP5, RRP6, RRP7, and RRP8) and two hormone-refractory human PCa tissues (TURP1 and TURP2). *Middle,* protein loading was monitored by Ponceau S staining of the PVDF membrane; *bottom,* IP with the anti-AR(441) antibody was performed to enrich the AR proteins and immunoblotted (*IB*) with anti-AR(N20) to detect the prototype AR, and AR-V7 by the anti-AR-V7 antibody. *D,* biochemical analysis of cellular localization of AR-V7 protein. VCaP and CWR22Rv1 cells were grown in phenol red–free RPMI 1640 containing CSS with or without 10 nmol/L R1881. The cytosolic fraction (*C*) and nuclear fraction (*N*) of lysates with equivalent number of cells were isolated and subjected to immunoblot analysis of AR-V7, prototype AR by anti-AR(N20) antibody, and β-actin.

(Fig. 2*C*), in 66 RRP cases for which long-term clinical follow-up data were available. In this same sample set (n = 66), higher prototype AR mRNA levels did not predict PSA failure (Supplementary Fig. S4*A*). Similarly, higher ratio of V7/AR did not predict PSA failure (Supplementary Fig. S4*B*), although there seemed to be a trend. AR-V1 expression was not associated with this clinical outcome (log-rank P = 0.498; data not shown). It is unknown why AR-V1 and AR-V7, although both overexpressed in HRPC specimens,

differed in their association with PSA recurrence. It is worth noting that our preliminary analysis predicted that AR-V1 variant-specific sequences (Fig. 1*A*) lack the basic amino acids characteristic of the bipartite nuclear localizing sequence (15) and therefore may not be a fully functional nuclear receptor (data not shown).

AR-V7 is translated and constitutively active. Transcript variants harboring PTC may be subjected to nonsense-mediated decay (16). Indeed, although similar transcript variants have been previously characterized for other steroid hormone receptor family members (17), no corresponding protein product has been reliably shown. Using the unique peptide sequence encoded by AR CE3, we generated polyclonal antibodies specifically against AR-V7. The antibodies recognized a single band of expected size (80 kDa) in VCaP and CWR22Rv1 cells (Fig. 3*A*), which expressed highest levels of AR-V7 mRNA (Supplementary Fig. S1). Similarly, AR-V7 protein was detected in protein extracts from these two cell lines that were enriched for AR proteins by IP with an antibody against the AR NTD (Fig. 3*B*). In addition, the antibody detected the AR-V7 antigen in two clinical HRPC specimens using both whole tissue lysates and IP concentrated extracts (Fig. 3*C*). Moreover, using IP concentrated protein extracts, we detected AR-V7 protein expression in 10 of 14 human PCa xenografts, 12 of which were derived from HRPC patients (18), but in only 1 of the 9 hormone-naive radical prostatectomy specimens (Supplementary Fig. S5). In CWR22Rv1 cells, small interfering RNA–mediated knockdown of AR-V7 expression or depletion of AR-V7 using anti-AR-V7 both resulted in significant reduction of the commonly observed ~80-kDa protein band but did not affect prototype AR expression (Supplementary Fig. S6), suggesting nearly equivalent AR-V7 and prototype AR protein levels in this cell line. Although the prototype AR responded to the treatment of androgen by localizing to the nucleus, a large fraction of endogenous AR-V7 was localized in

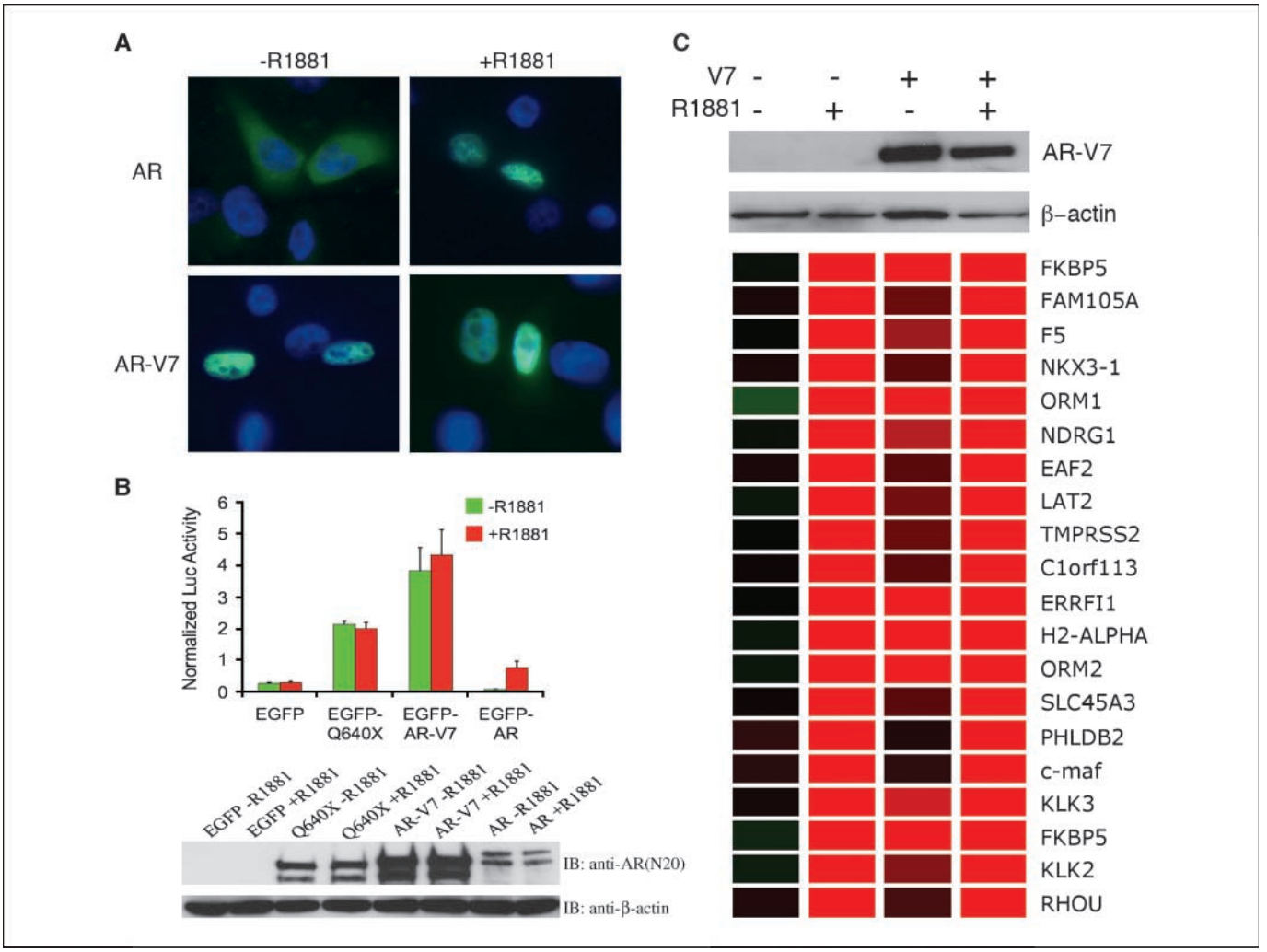

Figure 4. Constitutive function of AR-V7. *A,* constitutive nuclear localization of transfected AR-V7 in the absence of androgen. PC-3 cells were transfected with pEGFP-AR and pEGFP-AR-V7 to express the prototype AR or AR-V7 and examined for the localization of GFP-tagged AR proteins in the presence or absence of 5 nmol/L R1881. *B,* AR-V7 constitutively activates an AR luciferase reporter. PC-3 cells were transfected with vector control (*EGFP*), a LBD-truncated AR mutant (*EGFP-Q640X*), AR-V7 (*EGFP-AR-V7*), and prototype AR (*EGFP-AR*) and subjected to luciferase assays and Western blot analysis following culturing in the presence or absence of R1881. *C,* androgen-independent induction of AR-responsive genes by AR-V7 in LNCaP cells. LNCaP cells were transfected with pcDNA-AR-V7 to express the untagged AR-V7 protein or the control pcDNA vector and cultured with or without 10 nmol/L R1881 before being harvested for Western blot analysis or RNA extraction for expression microarray analysis. The genes shown were the top 20 ranked genes by fold induction following R1881 treatment in pcDNA empty vector–transfected LNCaP cells. Expression ratios of the test sample versus the common reference (pcDNA empty vector–transfected LNCaP without R1881) were represented by red (>1) and green colors (<1).

the nucleus in the absence of androgen and the proportion of nuclear AR-V7 did not change on androgen stimulation (Fig. 3*D*). The putative functional role of AR-V7 was investigated using exogenously transfected AR-V7 in AR-negative PC-3 cells. AR-V7 localized to the nucleus (Fig. 4*A*) and induced PSA reporter gene expression in an androgen-independent manner (Fig. 4*B*). Furthermore, in androgen-responsive LNCaP cells AR-V7 induced canonical androgen-responsive genes, such as *KLK3, KLK2, NKX3-1, FKBP5*, and *TMPRSS2*, in the absence of androgens, as shown by global gene expression analysis following transfection of the exogenous AR-V7 cDNA in LNCaP cells (Fig. 4*C*).

Hormonal therapy for advanced PCa is most commonly achieved by orchiectomy, systemic administration of LHRH agonists (e.g., leuprolide), and/or antiandrogens (e.g., bicalutamide). There are significant drawbacks associated with all existing androgen manipulation approaches. First, a variable period of clinical regression is followed by progression to HRPC, a lethal manifestation of the disease that is resistant to further therapies (4). Second, there are debilitating consequences from these treatments that must be considered when deciding whether and when to commence hormone therapy (2). Furthermore, sufficient levels of local androgens continue to be present in patients treated with combined androgen blockade (19). In spite of these challenges, hormone therapies remain the mainstay of treatment for patients with advanced PCa primarily due to the often dramatic clinical responses. The discovery of multiple LBD-truncated AR variants that mediate androgen-independent AR functions in HRPC and a subset of advanced but hormone-naive PCa adds another level of detail to the complex molecular mechanisms underlying the development of HRPC and may suggest new diagnostic and therapeutic approaches targeting this lethal disease. Indeed, these findings reinforce arguments for specific targeting of the AR NTD to achieve complete abrogation of AR signaling (20). Our quantitative mRNA data suggested that AR-V7 is a low-abundance variant relative to the prototype AR in the vast majority of clinical specimens, including HRPC (Supplementary Fig. S7). The relative contribution of the prototype AR and the less abundant yet androgen-independent AR variants to the development of HRPC is currently unknown and will require detailed investigation. Nevertheless, the detection of such variants in proper target tissues or cells, on further refinement of the detection methods, may predict or monitor hormone therapy efficacy and could potentially help guide the decision-making process about the type and timing of therapies given to patients with advanced PCa.

Disclosure of Potential Conflicts of Interest

No potential conflicts of interest were disclosed.

Acknowledgments

Received 7/20/2008; revised 10/5/2008; accepted 10/28/2008.

Grant support: David H. Koch Foundation. The Brady Urological Research Institute Prostate Specimen Repository is supported by the Prostate Specialized Program of Research Excellence grant (NIH/National Cancer Institute P50CA58236). J. Luo is a Phyllis and Brian L. Harvey Scholar, awarded by the Patrick C. Walsh Prostate Cancer Research Fund.

The costs of publication of this article were defrayed in part by the payment of page charges. This article must therefore be hereby marked *advertisement* in accordance with 18 U.S.C. Section 1734 solely to indicate this fact.

We thank Dr. Patrick Walsh, Sally Isaacs, and Kathleen Wiley for assistance with the clinical data; Dr. Angelo De Marzo and Helen Fedor for assisting with tissue preparation; Drs. Robert Getzenberg and John Isaacs for critical reading of the manuscript; Dr. Donald Coffey for insightful discussions; and Wasim Chowdhury for technical assistance.

References

1. Heinlein CA, Chang C. Androgen receptor in prostate cancer. Endocr Rev 2004;25:276–308.
2. Gelmann EP. Molecular biology of the androgen receptor. J Clin Oncol 2002;20:3001–15.
3. Shang Y, Myers M, Brown M. Formation of the androgen receptor transcription complex. Mol Cell 2002;9:601–10.
4. Armstrong AJ, Carducci MA. New drugs in prostate cancer. Curr Opin Urol 2006;16:138–45.
5. Scher HI, Sawyers CL. Biology of progressive, castration-resistant prostate cancer: directed therapies targeting the androgen-receptor signaling axis. J Clin Oncol 2005;23:8253–61.
6. Agoulnik IU, Weigel NL. Androgen receptor action in hormone-dependent and recurrent prostate cancer. J Cell Biochem 2006;99:362–72.
7. Céraline J, Cruchant MD, Erdmann E, et al. Constitutive activation of the androgen receptor by a point mutation in the hinge region: a new mechanism for androgen-independent growth in prostate cancer. Int J Cancer 2004;108:152.
8. Libertini SJ, Tepper CG, Rodriguez V, Asmuth DM, Kung HJ, Mudryj M. Evidence for calpain-mediated androgen receptor cleavage as a mechanism for androgen independence. Cancer Res 2007;67:9001–5.
9. Dehm SM, Schmidt LJ, Heemers HV, Vessella RL, Tindall DJ. Splicing of a novel androgen receptor exon generates a constitutively active androgen receptor that mediates prostate cancer therapy resistance. Cancer Res 2008;68:5469–77.
10. Luo J, Duggan DJ, Chen Y, et al. Human prostate cancer and benign prostatic hyperplasia: molecular dissection by gene expression profiling. Cancer Res 2001;61:4683–8.
11. Suzuki H, Freije D, Nusskern DR, et al. Interfocal heterogeneity of PTEN/MMAC1 gene alterations in multiple metastatic prostate cancer tissues. Cancer Res 1998;58:204–9.
12. Dhanasekaran SM, Barrette TR, Ghosh D, et al. Delineation of prognostic biomarkers in prostate cancer. Nature 2001;412:822–6.
13. Tepper CG, Boucher DL, Ryan PE, et al. Characterization of a novel androgen receptor mutation in a relapsed CWR22 prostate cancer xenograft and cell line. Cancer Res 2002;62:6606–14.
14. Quigley CA, Evans BA, Simental JA, et al. Complete androgen insensitivity due to deletion of exon C of the androgen receptor gene highlights the functional importance of the second zinc finger of the androgen receptor *in vivo*. Mol Endocrinol 1992;6:1103–12.
15. Zhou ZX, Sar M, Simental JA, Lane MV, Wilson EM. A ligand-dependent bipartite nuclear targeting signal in the human androgen receptor. Requirement for the DNA-binding domain and modulation by NH_2-terminal and carboxyl-terminal sequences. J Biol Chem 1994;269:13115–23.
16. Pan Q, Saltzman AL, Kim YK, et al. Quantitative microarray profiling provides evidence against widespread coupling of alternative splicing with nonsense-mediated mRNA decay to control gene expression. Genes Dev 2006;20:153–8.
17. Hirata S, Shoda T, Kato J, Hoshi K. Isoform/variant mRNAs for sex steroid hormone receptors in humans. Trends Endocrinol Metab 2003;14:124–9.
18. Saramäki OR, Porkka KP, Vessella RL, Visakorpi T. Genetic aberrations in prostate cancer by microarray analysis. Int J Cancer 2006;119:1322–9.
19. Montgomery RB, Mostaghel EA, Vessella R, et al. Maintenance of intratumoral androgens in metastatic prostate cancer: a mechanism for castration-resistant tumor growth. Cancer Res 2008;68:4447–54.
20. Dehm SM, Tindall DJ. Androgen receptor structural and functional elements: role and regulation in prostate cancer. Mol Endocrinol 2007;21:2855–63.

Ligand-Independent Androgen Receptor Variants Derived from Splicing of Cryptic Exons Signify Hormone-Refractory Prostate Cancer

Rong Hu, Thomas A. Dunn, Shuanzeng Wei, et al.

Cancer Res 2009;69:16-22.